

# Lawrence Berkeley National Laboratory

## Recent Work

### Title

OBSERVATION OF CORRELATION EFFECTS IN ZERO KINETIC ENERGY ELECTRON SPECTRA NEAR THE N1S AND C1S THRESHOLDS IN N<sub>2</sub>, CO, C<sub>6</sub>H<sub>6</sub>, AND C<sub>2</sub>H<sub>4</sub>

### Permalink

<https://escholarship.org/uc/item/12c0x4p9>

### Authors

Medhurst, L.J.

Ferrett, T.A.

Heimann, P.A.

### Publication Date

1988-05-01

e.2



# Lawrence Berkeley Laboratory

UNIVERSITY OF CALIFORNIA

## Materials & Chemical Sciences Division

Submitted to Journal of Chemical Physics

RECEIVED  
LAWRENCE  
BERKELEY LABORATORY

MAY 2 1988

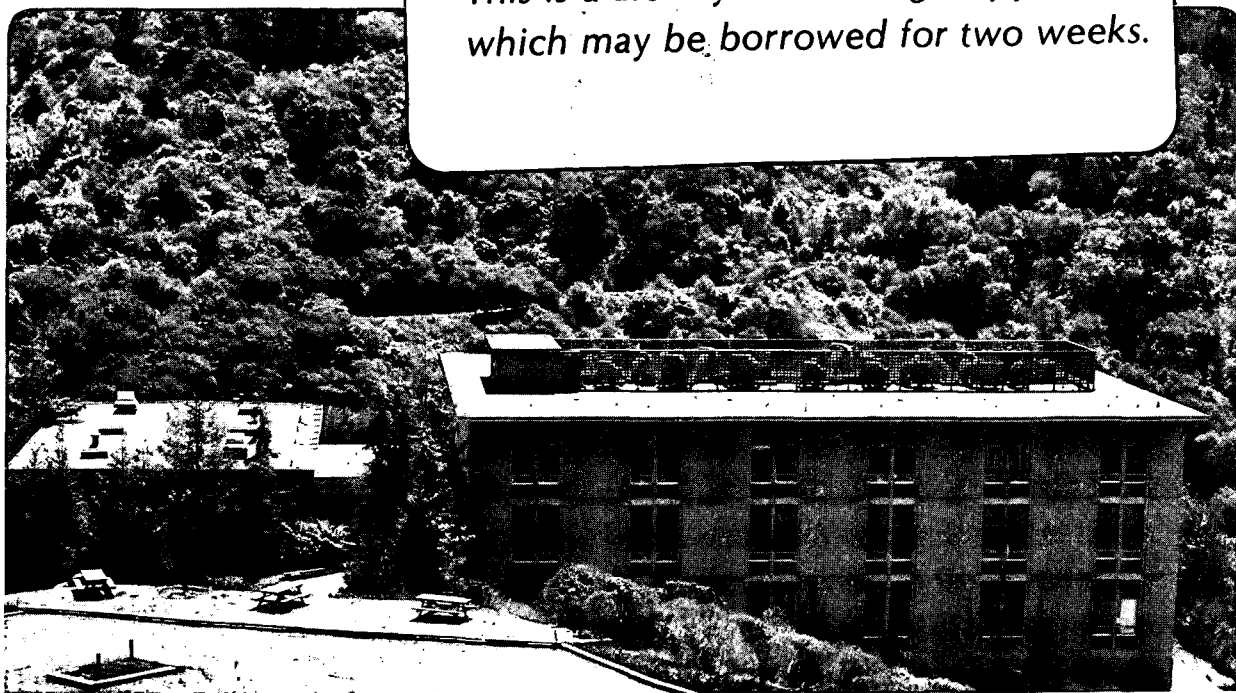
LIBRARY AND  
DOCUMENTS SECTION

### Observation of Correlation Effects in Zero Kinetic Energy Electron Spectra near the N1s and C1s Thresholds in N<sub>2</sub>, CO, C<sub>6</sub>H<sub>6</sub>, and C<sub>2</sub>H<sub>4</sub>

L.J. Medhurst, T.A. Ferrett, P.A. Heimann,  
D.W. Lindle, S.H. Liu, and D.A. Shirley

May 1988

**TWO-WEEK LOAN COPY**  
*This is a Library Circulating Copy  
which may be borrowed for two weeks.*



LBL-25263  
e.2

## **DISCLAIMER**

This document was prepared as an account of work sponsored by the United States Government. While this document is believed to contain correct information, neither the United States Government nor any agency thereof, nor the Regents of the University of California, nor any of their employees, makes any warranty, express or implied, or assumes any legal responsibility for the accuracy, completeness, or usefulness of any information, apparatus, product, or process disclosed, or represents that its use would not infringe privately owned rights. Reference herein to any specific commercial product, process, or service by its trade name, trademark, manufacturer, or otherwise, does not necessarily constitute or imply its endorsement, recommendation, or favoring by the United States Government or any agency thereof, or the Regents of the University of California. The views and opinions of authors expressed herein do not necessarily state or reflect those of the United States Government or any agency thereof or the Regents of the University of California.

OBSERVATION OF CORRELATION EFFECTS IN ZERO KINETIC ENERGY ELECTRON  
SPECTRA NEAR N1s AND Cls THRESHOLDS IN N<sub>2</sub>, CO, C<sub>6</sub>H<sub>6</sub> AND C<sub>2</sub>H<sub>4</sub>

L. J. Medhurst, T. A. Ferrett, P. A. Heimann, D. W. Lindle,  
S. H. Liu and D. A. Shirley

Department of Chemistry, University of California  
and  
Materials and Chemical Sciences Division  
Lawrence Berkeley Laboratory, 1 Cyclotron Road  
Berkeley, California 94720

May 1988

This work was supported by the Director, Office of Energy Research, Office of Basic Energy Sciences, Chemical Sciences Division of the U.S. Department of Energy under Contract No. DE-AC03-76SF00098. It was performed at the Stanford Synchrotron Radiation Laboratory, which is supported by the Department of Energy's Office of Basic Energy Sciences.

Observation of Correlation Effects in Zero Kinetic Energy

Electron Spectra Near the N1s and Cls Thresholds

in  $N_2$ , CO,  $C_6H_6$ , and  $C_2H_4$

L.J.Medhurst, T.A.Ferrett,\* P.A.Heimann<sup>†</sup>,

D.W.Lindle\*, S.H.Liu, D.A.Shirley

Department of Chemistry, University of California

and

Materials and Chemical Sciences Division

Lawrence Berkeley Laboratory, 1 Cyclotron Road

Berkeley, California 94720

Abstract: Zero kinetic energy (ZKE) spectra of  $N_2$ , CO,  $C_2H_4$ , and  $C_6H_6$  were taken across the N1s ( $N_2$ ) and Cls ionization thresholds. Discrete resonances at sub-threshold photon energies were observed and were found to become more intense as threshold is approached relative to the same peaks in absorption spectra. For  $N_2$  the satellite/main line branching ratios at threshold are: 11(1)% for the 419.7(1) eV binding energy satellite, and 2.3(1.0)% for the 426.5(1) eV binding energy satellite. For CO, the branching ratio for the 304.6(1) eV binding energy satellite is 15(2)% at its threshold. Branching ratios at threshold are also determined for the satellites of  $C_6H_6$  and  $C_2H_4$ . Decay characteristics

and assignments of the continuum features of  $C_6H_6$  and  $C_2H_4$  are also discussed.

---

\*Present address: National Bureau of Standards, Gaithersburg, MD 20899.

†Present address: Technische Universität München, D-8046 Garching b, München, Federal Republic of Germany.

## I. INTRODUCTION

Threshold photoelectron spectroscopy (TPES) has proved to be very powerful in the investigation of electron correlation phenomena in atoms.<sup>1-3</sup> In TPES a small electric field around the gas-photon interaction region extracts very low energy electrons, which are ejected as the photon energy is scanned across ionization thresholds. We shall refer to these as ZKE (zero kinetic energy) electrons, where confusion could otherwise result by using the word "threshold", which also refers specifically to the N1s or Cls main-line threshold itself. The spectra reported in this work are in fact ZKE spectra: that is, the signal carried by electrons of kinetic energy less than about 0.1 eV.

ZKE spectra can be used to determine the intensity of a correlation satellite<sup>4,5</sup> in the photoelectron spectrum, at its threshold relative to the intensity of the main line at its threshold. The simplest description of satellite intensities, the shake-up picture, based on time-dependent perturbation theory,<sup>4</sup> leads naturally to two limits. The sudden approximation describes the high-energy limit, with the photoelectron leaving so quickly that the satellite intensities are given by the overlap of the passive electrons. In this simple picture, the low-energy limit would have the photoelectron leaving so slowly that the passive electrons could follow the changing potential adiabatically, and satellite intensities would decrease more or less uniformly as the excitation energy decreased. However, recent atomic threshold and near-threshold photoelectron spectroscopy experiments have shown that the dependence of satellite intensities upon energy is actually quite

variable, implying the need for a more sophisticated theoretical approach.<sup>1-3,6</sup>

Even less is known about the intensity variation of satellites in molecules near threshold. Recently, the K-shell satellites of CO and N<sub>2</sub> have received much attention.<sup>6-9</sup> In both molecules, the lowest binding energy K-shell satellite appears to be enhanced near its threshold. The threshold photoelectron spectra of N<sub>2</sub> and CO, reported below, confirm these results, and the satellite intensities at threshold for C<sub>6</sub>H<sub>6</sub> and C<sub>2</sub>H<sub>4</sub> are also examined.

At incident photon energies above the main-line threshold, not only satellites contribute to the continuum absorption spectrum, but also shape resonances and discrete multi-electron resonances. In a threshold photoelectron spectrum only ZKE electrons are present, so that each main line gives one peak followed by its correlation satellite peaks. Also, although perhaps less obviously, discrete resonances, both above and below the main line threshold energy, produce ZKE electrons by the decay of the excited state through an Auger-like process, in which two or more electrons are ejected at once (double Auger decay). The great intensity of these peaks in the ZKE spectrum may arise through energy-sharing between the two emitted electrons in a way that favors low-energy electrons. Another channel that is expected to yield ZKE electrons is the decay of states reached by direct ionization, through shake-off processes.

Transitions through the above channels should lead to a ZKE spectral response that reflects much of the absorption spectrum. However, intensity increases due to classical one-electron shape



resonances in particular photoionization channels would not be prominent in the ZKE signal. Rather, peaks that are prominent in the ZKE spectrum above the main-line ionization threshold, if not due to correlation satellite state thresholds, should be assigned to doubly excited states. Thus, ZKE spectra can be used, with caution, to distinguish between shape resonances, which yield primarily single, higher-energy electrons, and doubly excited states, which decay by multielectron processes.<sup>10</sup> However, caution is required, because the ZKE signal may rise slightly at the shape resonance energy due to a double Auger decay branch.

The experiment is described briefly, then results for the four molecules are discussed successively. For each molecule, first we discuss the discrete resonance region below the main-line threshold, followed by the continuum region. Lastly we list our conclusions.

## II. EXPERIMENT

This experiment was performed at Stanford Synchrotron Radiation Laboratory operating in the 4x1 bunch mode on the four degree grazing incidence (grasshopper) monochromator on Beam Line III-1. For the N1s work (400-440eV) the resolution is ~0.9 eV FWHM. For the Cls work, the resolution is ~0.96 eV. The apparatus is described in detail elsewhere.<sup>10-12</sup> Briefly, the pulsed photon beam intersects an effusive gas beam defining an interaction region. A weak electric field extracts the electrons, which are energy analyzed by time-of-flight. The threshold electron analyzer uses space focusing conditions to improve its resolution, which is about 0.03 eV. At threshold, the entire  $4\pi$  solid angle is collected and the collection angle rapidly decreases for higher energy electrons. In this work only ZKE scans are reported. The

photon flux was monitored by a quartz window coated with sodium salicylate. The response as a function of photon energy was calibrated using the known cross section of argon and neon, as has previously been done for lower photon energies.<sup>13</sup> A least squares fitting routine was used to fit the spectra. All parameters, mean energy, width and intensity were allowed to vary independently. Gaussian functions were used to fit peaks corresponding to discrete resonances. A constant function and a gaussian convoluted with a step function centered over the 1s ionization threshold, to model shake-off, were used to fit the background.

The 1s main line peaks, because of their asymmetric profiles, were fitted with a Niehaus' function<sup>14</sup> convoluted with a gaussian. This is the result of post collision interaction (PCI), which is well characterized in atoms. In Niehaus' semiclassical model,<sup>14</sup> the low energy photoelectron is overtaken by the faster Auger electron. This causes an abrupt change in the potential of both electrons, increasing the kinetic energy of the Auger electron and decreasing the kinetic energy of the photoelectron. The function derived by Niehaus, with a natural lifetime taken from the measured core hole lifetime convoluted with a gaussian of the monochromator bandpass, was used to fit the 1s ionization peak. This resulted in a significantly larger intensity for this peak than a simple gaussian function and shifted the maximum peak intensity to higher photon energy. The satellite peaks should also exhibit an asymmetric profile due to PCI. In general, some other line broadening process made it impossible to differentiate between the Niehaus-gaussian function and a simple gaussian function, so gaussian

functions were used to fit the satellite peaks. Relative intensities of continuum features are scaled to the  $1s$  ionization intensity at the photon energy of that feature. Reported uncertainties are statistical; systematic errors are estimated to be less than 10%.

### III. RESULTS

#### A. NITROGEN

The ZKE photoelectron spectrum of nitrogen is shown in Fig. 1 along with the EELS spectrum of Wight et. al.<sup>15</sup> over the same energy range.

##### 1. Discrete Resonances

Peaks labeled 1 through 4 in Fig. 1 are the below-threshold peaks which arise from excitations to discrete states. Table I lists the energies, transition assignments, and relative intensities of these features. Also listed in Table I are the high resolution EELS results of Tronc et. al.<sup>16</sup> for comparison. A prominent  $1s \rightarrow \pi^*$  resonance and Rydberg transitions leading to ionization are present in both the EELS spectrum and the threshold spectrum. The assignments in Table I were made by Tronc et. al., who used a combination of multiquantum defect theory and the equivalent core model in their interpretation, with the dominant Rydberg transitions being the  $np$  series. Table I shows that the relative intensities of the transitions to higher  $n$  states are larger in the ZKE spectrum than in the EELS spectrum. In fact, the unresolved group, peak 4, has almost four times greater intensity compared to the  $1s \rightarrow \pi^*$  transition, than the sum of the same peaks from the EELS work Tronc et. al. This result is analogous to the atomic case,

where relative probability for an excited state to undergo shake-off increases with greater  $n$ .<sup>1</sup>

## 2. Continuum Features

Figure 2 contains the ZKE spectrum for  $N_2$  and the 1487 eV PES spectrum of Gelius et. al.<sup>5</sup> The results for the continuum features are presented in Table II, along with the Al  $K\alpha$  (1487eV PES) results of Gelius et. al.<sup>5</sup> Peak 5 is due to the onset of N1s ionization. Peak 6 in the ZKE photoelectron spectrum is assigned, on the basis of its energy, to a doubly excited state, of the type  $1s^{-1}val^{-1}\pi^*$  Ryd, which could decay through channels yielding low-energy electrons. Because of its prominent appearance in the threshold spectrum, this peak is not assigned as a N1s shape resonance, and its binding energy is too low for a N1s satellite. The more symmetric line shape and the similarity in shape and relative intensity to the corresponding peak in the EELS spectrum are typical of discrete resonances in threshold spectra.

A  $N_2 \sigma^*$  shape resonance has been observed at 419 eV in both the EELS spectrum and by direct phototemission in the N1s main line.<sup>17</sup> The first N1s satellite peak, assigned as  $1s^{-1}\pi^{-1}\pi^*$ , was reported by Gelius et. al.<sup>5</sup> to lie at 419.2 eV. Either of these would be candidate assignments for peak 7, if energy were the sole criterion. However, other criteria strongly favor the  $1s^{-1}\pi^{-1}\pi^*$  satellite assignment. The satellite threshold should yield ZKE electrons, while there is no reason to expect a shape resonance to yield ZKE electrons. Also, Kerkhoff et. al.<sup>18</sup> have measured the cross section for the N1s satellites as a function of photon energy. Their results indicate an increase in the relative cross section close to threshold for the 419 eV binding energy

satellite. At the Al  $K\alpha$  (1487 eV) photon energy, the intensity of this peak relative to the of N1s main line is 2.1%, whereas at its threshold, it is 11% as intense as the N1s peak. This factor of five is in qualitative agreement with the results reported by Ungier and Thomas<sup>7</sup> using Ti  $L\alpha$  (452 eV) radiation.

Peak 8 at 426.5 eV is assigned as the second satellite of 425.9 eV known binding energy. The difference in reported binding energy between the threshold results and the Al  $K\alpha$  results is probably due to a PCI shift of the maximum intensity of the satellite peaks to higher photon energy. Its intensity at its threshold, relative to the N1s main line at the same photon energy, is approximately ten times smaller than at 1487 eV photon energy. This satellite has been assigned, through CI calculations as  $\pi, \pi^*$  singlet paired  $1s^{-1}\pi^{-1}\pi^*$  mixed with  $1s^{-1}\pi^{-2}\pi^*2, 9, 19-21$

The near degeneracy in energy of the  $\sigma_u$  shape resonance in the N1s ionization partial cross section to the binding energy of the first satellite suggests that it could lend intensity to this satellite, such as has been confirmed both theoretically and experimentally for satellites in the inner valence region.<sup>22</sup> The 419.7 eV binding energy peak is, however, more than twice as broad as the N1s main line peak width, which is mostly instrumental. Therefore both satellite peaks may contain transitions to more than one electronic state.

The  $N_2$  threshold spectrum above 430 eV appears to contain structure qualitatively similar to the Al  $K\alpha$  satellite spectrum. Although the statistical accuracy is marginal, a doublet structure may be present

near 435 eV, and the continuum baseline appears to rise before 440 eV, perhaps due to shake-off processes.

## B. CARBON MONOXIDE

The ZKE photoelectron spectrum of CO across the Cls ionization threshold is presented in Fig. 3 along with the EELS spectrum of Wight et. al.<sup>15</sup> for the same range.

### 1. Discrete Resonances

The discrete part of the spectrum is summarized in Table III, and compared with the results of Tronc et. al.<sup>23</sup> Again the  $1s \rightarrow \pi^*$  resonance is well resolved, and followed by unresolved transitions to Rydberg states. The transitions were assigned in the same manner as for isoelectronic  $N_2$ . Just as with nitrogen and the atomic case, the transitions to higher n-states seem to produce more shake-off through ZKE electrons.

### 2. Continuum Features

The ZKE phototelectron spectrum of CO above the Cls threshold, presented in Fig. 4 along with the 1487 eV PES results of Gelius et. al.,<sup>5</sup> is similar to that of isoelectronic  $N_2$ . The continuum results are presented in Table IV. Peak 5, the main line, is due to ionization of the carbon 1s electron. Peak 6 is assigned to a doubly excited state of the type  $1s^{-1} val^{-1} \pi^* Ryd$  as in nitrogen, and a broad  $\sigma^*$  shape resonance centered at 303 eV in the EELS spectrum is absent in the threshold spectrum, as expected.

Since CO is isoelectronic with  $N_2$ , the electronic assignments for the satellites are similar.<sup>5,6,24</sup> The first satellite, peak 7, is

enhanced by nearly a factor of five relative to the 1s main line, when compared to the ratio at 1487 eV photon energy.

The second satellite in the Al K $\alpha$  photoelectron spectrum of Gelius et. al.<sup>5</sup> would appear at 311 eV photon energy in the ZKE spectrum. Since there is no peak apparent at this energy, its intensity is estimated to be less than 2% of the 1s main line intensity. This is in qualitative agreement with the experimental results of Reiner et. al.,<sup>6</sup> who found the intensity of the first satellite of CO to increase, and the second satellite to decrease relative to 1s ionization with decreasing photon energy.

However, there is a small shoulder in the ZKE spectrum on the higher binding energy side of the first satellite, but well below the second satellite's binding energy. It is unlikely that this is part of a vibrational envelope, as the combined peak width is over 3 eV, and the shape is indicative of a second peak. This second peak might correspond to the satellite states of  $2\Sigma^-$  and  $2\Delta$  symmetry, which should lie between 305.7 and 307.4 eV binding energy, as calculated by Schirmer et. al.,<sup>9</sup> using a Green's function technique. If this interpretation is correct, this new result for satellites in core-level molecular satellite spectroscopy is similar to recent findings for rare-gas atoms, at<sup>3</sup> and near<sup>25</sup> ZKE. The result is that new satellites appear in the ZKE spectrum which are absent in the sudden limit. Electron correlation effects (e.g. interchannel coupling) are presumed responsible for their appearance near ZKE even though they are disfavored by symmetry in the absence of interchannel coupling, in high energy photoelectron spectra. One explanation for the increased intensity of the lowest binding energy

satellites in  $N_2$  and CO is that the satellites with thresholds near the  $\sigma^*$  shape resonance can borrow intensity from that shape resonance, as suggested by Reimer et. al.<sup>6</sup> With the current resolution, however, it is difficult to say conclusively which satellites are responsible for this enhancement, but more than one electronic state appears to be involved.

### C. BENZENE

Figure 5 shows the ZKE photoelectron spectrum of benzene and the EELS spectrum of Hitchcock et. al.<sup>26</sup> over the same energy range.

#### 1. Discrete Resonances

The results for the discrete resonances of benzene are listed in Table V. The asymmetric profile of the  $1s \rightarrow \pi^*$  resonance, peak 1, is most likely due to an unresolved vibrational envelope. Qualitatively, it appears that the resonances to higher np states again produce more shake-off to ZKE electron channels.

#### 2. Continuum Features

Figure 6 shows the  $C_6H_6$  ZKE spectrum above the Cls threshold, together with a PES spectrum from Ohta et. al. Peak 5 corresponds to the Cls main line. It shows the characteristic line shape caused by PCI. There has been some controversy over the assignments of the other continuum features. On the basis of MS- $X\alpha$  calculations, Horsley et. al.<sup>27</sup> have assigned both resonances in the EELS spectrum at 293.5 and 300 eV (see Fig. 5) to molecular shape resonances. Piancastelli et. al.<sup>28</sup> have assigned these resonances on the basis of their decay characteristics. The peak at 293.5 eV was not evident in the Cls cross



section, and was therefore deduced to decay primarily through many electron channels. The 300 eV peak was found to decay primarily by  $1s$  ionization. A partially resolved peak near 293.5 eV is observed in the ZKE spectrum but a 300 eV peak is not; this is consistent with the conclusion of Piancastelli et. al.: peak 6 can be a doubly excited state of the form  $1s^{-1}val^{-1}\pi^*$  Ryd, rather than a  $\sigma^*$  shape resonance. The absence of a peak at 300 eV also tends to confirm their conclusion that there is a shape resonance with a maximum at 300 eV.

The high background makes the continuum results uncertain. Peak 7 is relatively well resolved. Compared to the results of Ohta et al.<sup>29</sup> (i.e. comparable resolution), the relative intensity is the same at ZKE as at 1487 eV photon energy. The second satellite peak, peak 8, tentatively appears present and enhanced at ZKE.

#### D. ETHYLENE

The ZKE photoelectron spectrum of ethylene and the EELS spectrum of Hitchcock et. al.<sup>26</sup> are presented in Fig. 7.

##### 1. Discrete Resonances

The discrete resonances of ethylene are listed in Table VII. The slightly asymmetric profile of the first resonance,  $1s \rightarrow \pi^*$ , is probably caused by transitions to unresolved vibrational states, and again the Rydberg peaks which correspond to higher  $n$  transitions seem to produce more threshold electrons compared to the  $1s \rightarrow \pi^*$  resonance.

##### 2. Continuum Features

Continuum resonance results are summarized in Table VIII. The Cls main line peak, peak 5, exhibits the characteristic asymmetry due to PCI. The peak at 293.5 eV in the EELS spectrum, peak 6, is obscured by

the PCI broadened tail of peak 5; however, it appears that there may be some intensity at this photon energy in the ZKE spectrum. The resonance at 295.5 eV appears to be weakly present, as peak 7, in the ZKE spectrum. This gives tentative, but far from conclusive, support to the conclusion of Piancastelli et. al., that this peak in the EELS spectrum is a doubly excited state. The next two peaks in the continuum spectrum are assigned to satellites. A satellite at the energy of peak 9 has been seen before.<sup>28</sup> The maxima in the ZKE spectrum near 303 eV and 307 eV indicate that higher binding energy satellites could also be present.

#### IV. CONCLUSIONS

The threshold electron studies reported above have revealed these new insights about the behavior of molecular resonances and satellites near a K-shell threshold:

1. In all four molecules, discrete-state resonances below threshold, observed earlier in EELS work, also appeared in the ZKE spectra. This indicates decay through double-ionization channels, which can produce ZKE "shake-off" electrons. Furthermore, in progressing from the lowest-energy resonance peak up toward threshold, the ZKE peak intensity ratios increased relative to the EELS peak intensity ratios. This indicates that the ZKE channels become relatively more important for higher Rydberg levels.

2. In CO and N<sub>2</sub> the lowest binding energy Cls and Nls satellites at 304.5 eV and 419.2 eV, respectively, were dramatically enhanced to five times the sudden limit relative intensity near threshold. The widths of these peaks, and especially the high energy shoulder on the CO Cls

satellite, indicate that more than one electronic state is included in the satellite peak at threshold. In  $C_6H_6$  the lowest energy satellite, at 299 eV, is not enhanced at threshold, but the higher energy satellite at 302 eV is.

3. The low-energy resonances in the EELS spectra, at 293.5 eV in  $C_6H_6$  and 295.5 eV in  $C_2H_4$ , decay through ZKE channels and are therefore most probably due to doubly excited states rather than  $\sigma^*$  shape resonances.

4. In general, multi-electron (correlation) effects were found to contribute significantly to the EELS spectrum. As the ionization threshold for a core level molecular orbital is approached from above or below, multi-electron effects increase, manifesting themselves in the ZKE spectra of Rydberg peaks below threshold and satellite peaks above.

Finally, zero kinetic energy photoelectron spectroscopy can provide unique insights into electron correlation effects at energies near core-levels thresholds.

## References:

1. P. A. Heimann, U. Becker, H. G. Kerkhoff, B. Langer, D. Szostak, R. Wehlitz, D. W. Lindle, T. A. Ferrett, and D. A. Shirley, Phys. Rev. A 34, 3782 (1986).
2. P. A. Heimann, D. W. Lindle, T. A. Ferrett, S. H. Liu, L. J. Medhurst, M. N. Piancastelli, D. A. Shirley, U. Becker, H. G. Kerkhoff, B. Langer, D. Szostak and R. Wehlitz, J. Phys. B: At. Mol. Phys. 20, 5005 (1987).
3. U. Becker, B. Langer, H. G. Kerkhoff, M. Kupsch, D. Szostak, R. Wehlitz, P. A. Heimann, S. H. Liu, D. W. Lindle, T. A. Ferrett, and D. A. Shirley, Phys. Rev. Lett., in press.
4. T. Åberg, Phys. Rev. 156, 35 (1967).
5. U. Gelius, J. Electron Spectros. Relat. Phenom. 5, 985 (1974).
6. A. Reimer, J. Schirmer, J. Feldhaus, A. M. Bradshaw, U. Becker, H. G. Kerkhoff, B. Langer, D. Szostak, and R. Wehlitz, Phys. Rev. Lett. 57, 1707 (1986).
7. L. Ungier and T. D. Thomas, Phys. Rev. Lett. 53, 435 (1984).
8. T. D. Thomas, Phys. Rev. Lett. 52, 417 (1984).
9. J. Schirmer, G. Angonoa, and L. S. Cederbaum, Z. Phys. D. 5, 253 (1987).
10. M. N. Piancastelli, D. W. Lindle, T. A. Ferrett, and D. A. Shirley, J. Chem Phys. 86(5) 2765 (1987).
11. M. G. White, R. A. Rosenberg, G. Gabor, E. D. Poliakoff, G. Thornton, S. H. Southworth and D. A. Shirley, Rev. Sci Instr. 50, 1268 (1979).
12. P. A. Heimann, PhD Thesis, University of California, Berkeley. LBL#22419 (1987).
13. D. W. Lindle, T. A. Ferrett, P. A. Heimann, and D. A. Shirley, Phys. Rev. A 34, 1131 (1986).
14. A. Niehaus, J. Phys. B: At. Mol. Phys. 19 911 (1977).
15. G. R. Wight, C. E. Brion and M. J. Van der Wiel, J. Electron Spectrosc. Relat. Phenom. 1, 457 (1972/73).
16. M. Tronc, G. C. King and F. H. Read, J. Phys. B: At. Mol. Phys. 13 (1980) 999-1008.

17. D. W. Lindle, C. M. Truesdale, P. H. Kobrin, T. A. Ferrett, P. A. Heimann, U. Becker, H. G. Kerkhoff, and D. A. Shirley, *J. Chem. Phys.* **81**, 5375 (1984).
18. J. Feldhaus, A. Reimer, J. Schirmer, A. M. Bradshaw, U. Becker, H. G. Kerkhoff, B. Langer, D. Szostak, R. Wehlitz, and W. Braun, Fourteenth International Conference on X-ray and Inner-shell Processes Program and Abstracts (1987).
19. W. R. Rodwell, M. F. Guest, T. Darko, I. H. Hillier and J. Kendrick, *Chem. Phys.* **22** (1977) 467-473.
20. W. Butscher, R. J. Buenker, and S. D. Peyerimhoff, *Chem. Phys. Lett.* **52**, 449 (1977).
21. H. Ågren, R. Arneberg, J. Muller, and R. Manne, *Chemn. Phys.* **83**, 53 (1984).
22. P. Langhoff, S. R. Langhoff, T. N. Rescigno, J. Schirmer, L. S. Cederbaum, W. Domcke, and W. Von Niessen, *Chem Phys.* **58** (1981) 71-91.
23. M. Tronc, G. c. King, and F. H. Read, *J Phys. B: At. Mol. Phys.* **12** (1979) 137.
24. M. F. Guest, W. R. Rodwell, T. Darko, I. H. Hillier and J. Kendrick, *J. Chem. Phys.* **66**, 5447 (1977).
25. C. E. Brion, A. O. Bawagan, and K. H. Tan, *Chem Phys. Lett.* **13**, 76, (1987).
26. A. P. Hitchcock and C. E. Brion, *J. Electron Spectrosc. Relat. Phenom.* **10**, 317 (1977).
27. J. A. Horsley, J. Stohr, A. P. Hitchcock, D. C. Newbury, A. K. Johnson, and F. Sette, *J. Chem. Phys.* **83**, 6099 (1985).
28. M. N. Piancastelli, T. A. Ferrett, D. W. Lindle, L. J. Medhurst, P. A. Heimann, S. H. Liu, and D. A. Shirley, in press.
29. T. Ohta, T. Fujikawa and H. Kuroda, *Chem Phys. Lett.* **32**, 369 (1975).

Table I: Discrete Resonances in N<sub>2</sub>

Peak	Assignment	Threshold PES		EELS <sup>a</sup>	
		Energy	Relative Intensity	Energy <sup>b</sup>	Relative Intensity
1	1s <sup>-1</sup> π*	400.9(1)	100%	400.86(3)	100%
2	1s <sup>-1</sup> 3s	406.2(1)	2.8(8)%	402.29(3)	1.2(1)%
3	1s <sup>-1</sup> 3p	407.1(1)	4.3(6)%	407.18(1)	2.9(3)%
4	1s <sup>-1</sup> 3d	408.7(3)	13.6(6)%	408.4(1)	1.1(1)%
	1s <sup>-1</sup> 4p			409.12(2)	0.6(1)%
	1s <sup>-1</sup> 5p			409.49(2)	0.6(1)%
	1s <sup>-1</sup> 6p			409.78(2)	0.4(1)%

<sup>a</sup>Tronc et. al. <sup>13</sup><sup>b</sup>Energy is for v= 0 transition

Table II: Continuum Resonances in N<sub>2</sub>

Peak	Assignment	Threshold PES		Al K $\alpha^a$ (PES)	
		Energy	Relative Intensity	Energy	Relative Intensity
5	$1s^{-1}$	409.7(1)	100%	409.86(3)	100%
6	$1s^{-1}val^{-1}\pi^*Ryd$	414.9(1)			
7	$1s^{-1}\pi^{-1}\pi^*$	419.7(1)	11(1)% <sup>b</sup>	419.2	2.1%
8	$1s^{-1}\pi^{-1}\pi^{*c}$	426.5(1)	2.3(1.0) <sup>b</sup> %	425.9	24.6%
	$1s^{-1}\pi^{-2}\pi^{*2}$				

<sup>a</sup>Gelius et. al. <sup>5</sup>

<sup>b</sup>Relative intensities are scaled to the  $1s^{-1}$  intensity at the photon energy of the satellite's threshold.

<sup>c</sup> $\pi$  electron and  $\pi^*$  electron are singlet paired.<sup>14</sup>

Table III: Discrete Resonances in CO

Peak	Assignment	Threshold PES		EELS <sup>a</sup>	
		Energy	Relative Intensity	Energy <sup>b</sup>	Relative Intensity
1	$1s^{-1}\pi^*$	287.4(1)	100%	284.40(2)	100%
2	$1s^{-1}3s$	292.1(1)	2.4(2)%	292.37(2)	1.5(3)%
3	$1s^{-1}3p$	293.4(1)	12.2(9)%	293.33(4)	5(1)%
4	$1s^{-1}3d$	295.1(6)	9.9(7)%	294.60(3)	0.35(9)%
	$1s^{-1}4p$			294.77(3)	1.3(3)%
	$1s^{-1}5p$			295.30(3)	0.35(9)%
	$1s^{-1}6p$			295.59(3)	0.53(18)%

<sup>a</sup>Tronc et. al. <sup>16</sup><sup>b</sup>Energy is for  $v=0$  transition



Table IV: Continuum Resonances in CO

Peak	Assignment	Threshold PES		Al $K\alpha^a$ (PES)	
		Energy	Relative Intensity	Energy	Relative Intensity
5	$1s^{-1}$	296.2(1)	100%	296.2	100%
6	$1s^{-1}val^{-1}\pi^*$ Ryd	301.5(1)			
7	$1s^{-1}\pi^{-1}\pi^*$	304.6(1)	15(2)% <sup>b</sup>	304.5	3.1%
8		306.9(1)	5(1)% <sup>b</sup>		
	$1s^{-1}\pi^{-1}\pi^{*c}$ $1s^{-1}\pi^{-2}\pi^{*2}$			311.1	5.6%

<sup>a</sup>Gelius et. al. <sup>5</sup>

<sup>b</sup>Relative intensities are scaled to the  $1s^{-1}$  intensity at the photon energy of the satellite's threshold.

<sup>c</sup> $\pi$  electron and  $\pi^*$  electron are singlet paired.<sup>17</sup>

Table V: Discrete Resonances in C<sub>6</sub>H<sub>6</sub>

Peak	Assignment	Threshold PES		EELS <sup>a</sup>
		Energy	Relative Intensity	Energy
1	1s <sup>-1</sup> π*	285.2(1)	100%	285.2(1)
2	1s <sup>-1</sup> 3s	287.2(1)	20(1)%	287.2(1)
3	1s <sup>-1</sup> 3p	287.9(1)	18(2)%	288.0(1)
	1s <sup>-1</sup> 3d			288.6(1)
4	1s <sup>-1</sup> 4s	289.0(1)	62(2)%	288.9(1)

<sup>a</sup>Hitchcock et. al. <sup>18</sup>

Table VI: Continuum Resonances in C<sub>6</sub>H<sub>6</sub>

Peak	Assignment	Threshold PES		Al K $\alpha^a$ (PES)	
		Energy	Relative Intensity	Energy	Relative Intensity
5	$1s^{-1}$	290.3(1)	100%	290.42	100%
6	$1s^{-1}val^{-1}\pi^*Ryd$	293.5(1)			
7	$1s^{-1}\pi^{-1}\pi^*$	299(1)	10(4)% <sup>b</sup>	297.4	10.5%
8	$1s^{-1}\pi^{-1}\pi^*$	302(1)	16(8)% <sup>b</sup>	301.3	2.5%

<sup>a</sup>Ohta et. al. <sup>27</sup>

<sup>b</sup>Relative intensities are scaled to the  $1s^{-1}$  intensity at the photon energy of the satellite's threshold.

Table VII: Discrete Resonances in C<sub>2</sub>H<sub>4</sub>

Peak	Assignment	Threshold PES		EELS <sup>a</sup>
		Energy	Relative Intensity	Energy <sup>b</sup>
1	1s <sup>-1</sup> π*	284.8(1)	100%	284.67(3)
	1s <sup>-1</sup> 3s			287.24(3)
2	1s <sup>-1</sup> 3p	288.0(1)	91(3)%	287.88(3)
3	1s <sup>-1</sup> 4p	289.3(1)	40(3)%	289.40(4)
4	1s <sup>-1</sup> 5p	290.0(1)	37(3)%	289.94(1)

<sup>a</sup>Tronc et. al. <sup>16</sup>

<sup>b</sup>Energy is for v= 0 transition.

Table VIII: Continuum Resonances in C<sub>2</sub>H<sub>4</sub>

Peak	Assignment	Threshold PES		EELS <sup>a</sup>
		Energy	Relative Intensity	Energy
5	1s <sup>-1</sup>	290.8(1)	100%	290.74(4)
6	1s <sup>-1</sup> val <sup>-1</sup> π*Ryd	292.7(1)		
7	1s <sup>-1</sup> val <sup>-1</sup> RydRyd	295.6(1)		
8	1s <sup>-1</sup> val <sup>-1</sup> Ryd	298.2(1)	1.5(3)% <sup>b</sup>	
9	1s <sup>-1</sup> val <sup>-1</sup> Ryd	299.7(1)	2.2(3)% <sup>b</sup>	

<sup>a</sup>Tronc et. al. <sup>16</sup>

<sup>b</sup>Relative intensities are scaled to the 1s<sup>-1</sup> intensity at the photon energy of the satellite's threshold.

## Figure Captions

- Figure 1: ZKE scan of  $N_2$  from 397 to 440 eV photon energy. The solid line is a least squares fit to the spectrum. Included for comparison is the EELS spectrum of Wight et. al.<sup>15</sup>
- Figure 2: ZKE scan of  $N_2$  above the N1s threshold. The solid line is a least squares fit to the spectrum. Included for comparison is the PES spectrum of Gelius et. al.<sup>5</sup>
- Figure 3: ZKE scan of CO from 285 to 320 eV photon energy. The solid line is a least squares fit to the spectrum. Included for comparison is the EELS spectrum of Wight et. al.<sup>15</sup>
- Figure 4: ZKE scan of CO above the Cls threshold. The solid line is a least squares fit to the spectrum. Included for comparison is the PES spectrum of Gelius et. al.<sup>5</sup>
- Figure 5: ZKE scan of  $C_6H_6$  from 280 to 312 eV photon energy. The solid line is a least squares fit to the spectrum. Included for comparison is the EELS spectrum of Hitchcock et. al.<sup>24</sup>
- Figure 6: ZKE scan of  $C_6H_6$  above the Cls threshold. The solid line is a least squares fit to the spectrum. Included for comparison is the PES spectrum of Ohta et. al.<sup>26</sup>
- Figure 7: ZKE scan of  $C_2H_4$  from 280 to 312 eV photon energy. The solid line is a least squares fit to the spectrum. Included for comparison is the EELS spectrum of Hitchcock et. al.<sup>24</sup>

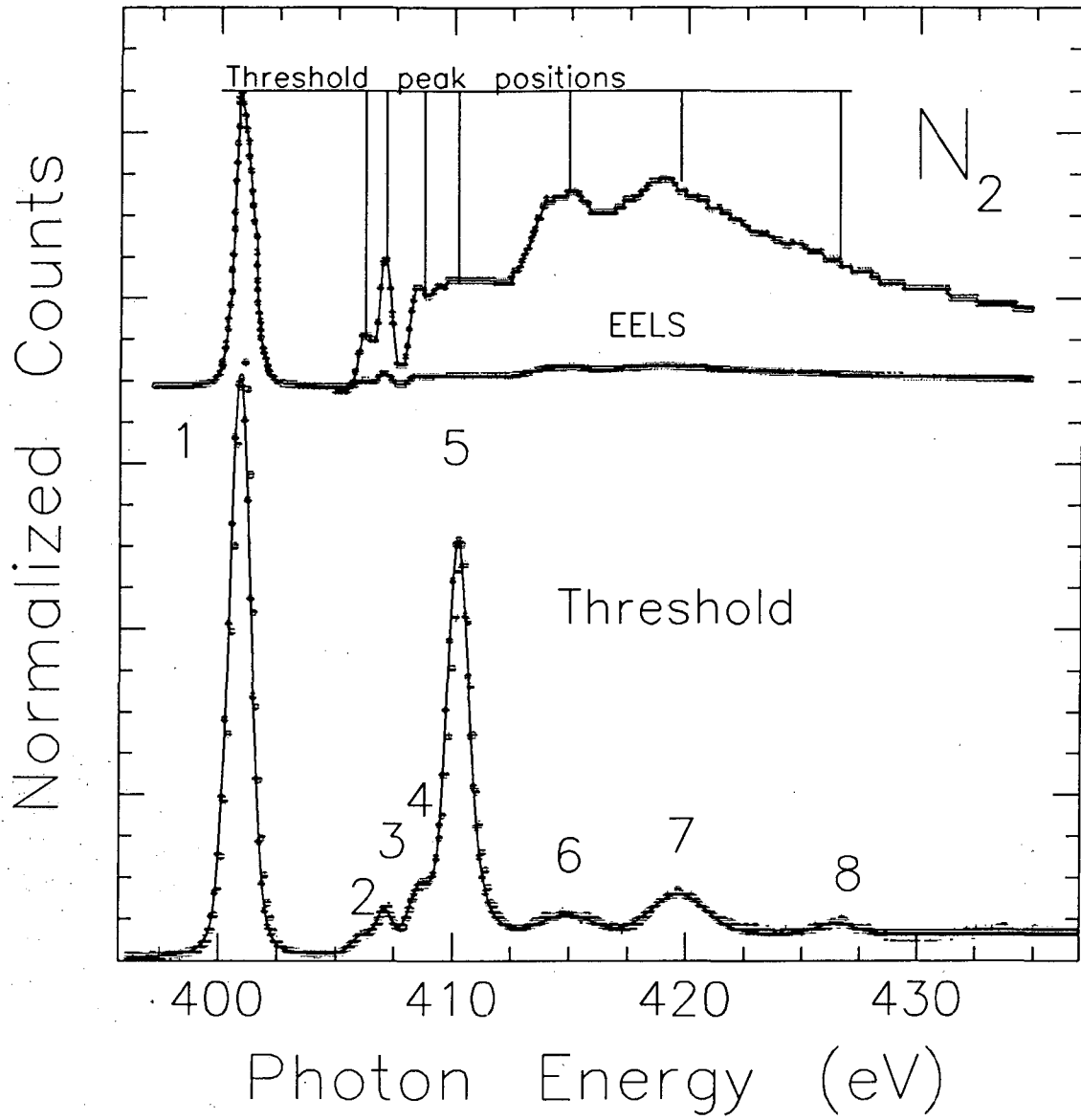


Figure 1

XBL 885-1916

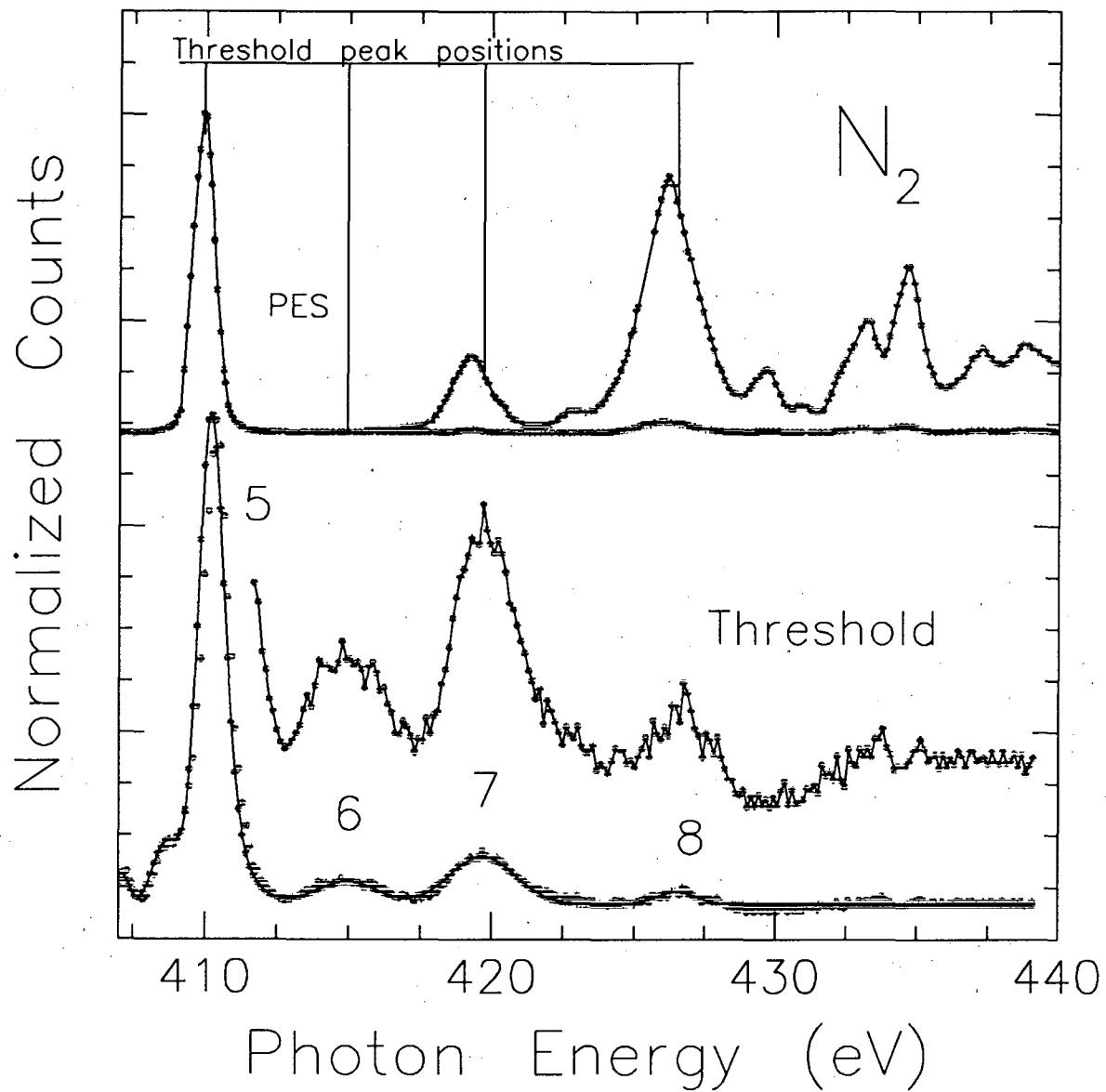


Figure 2

XBL 885-1917



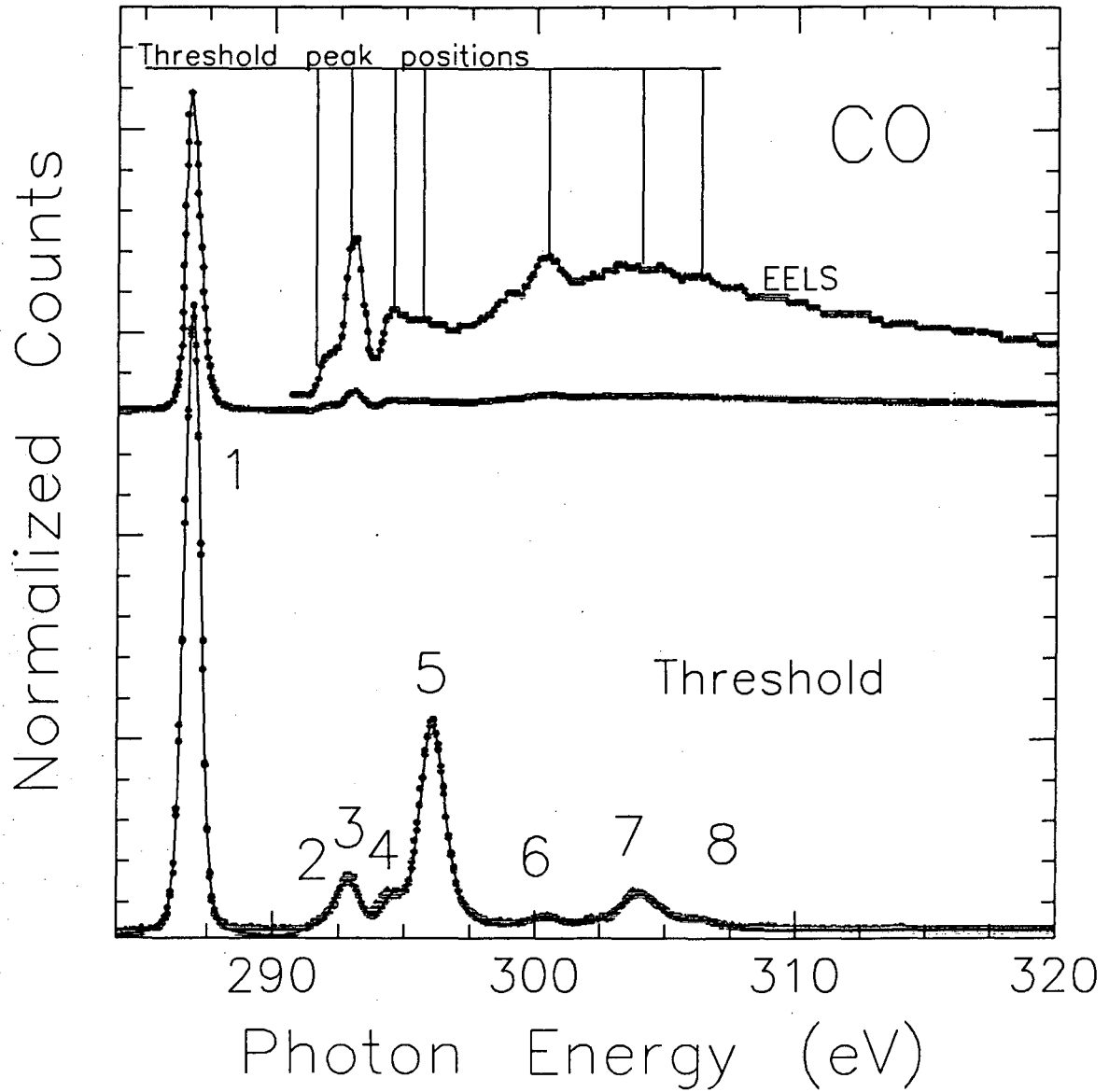


Figure 3

XBL 885-1918

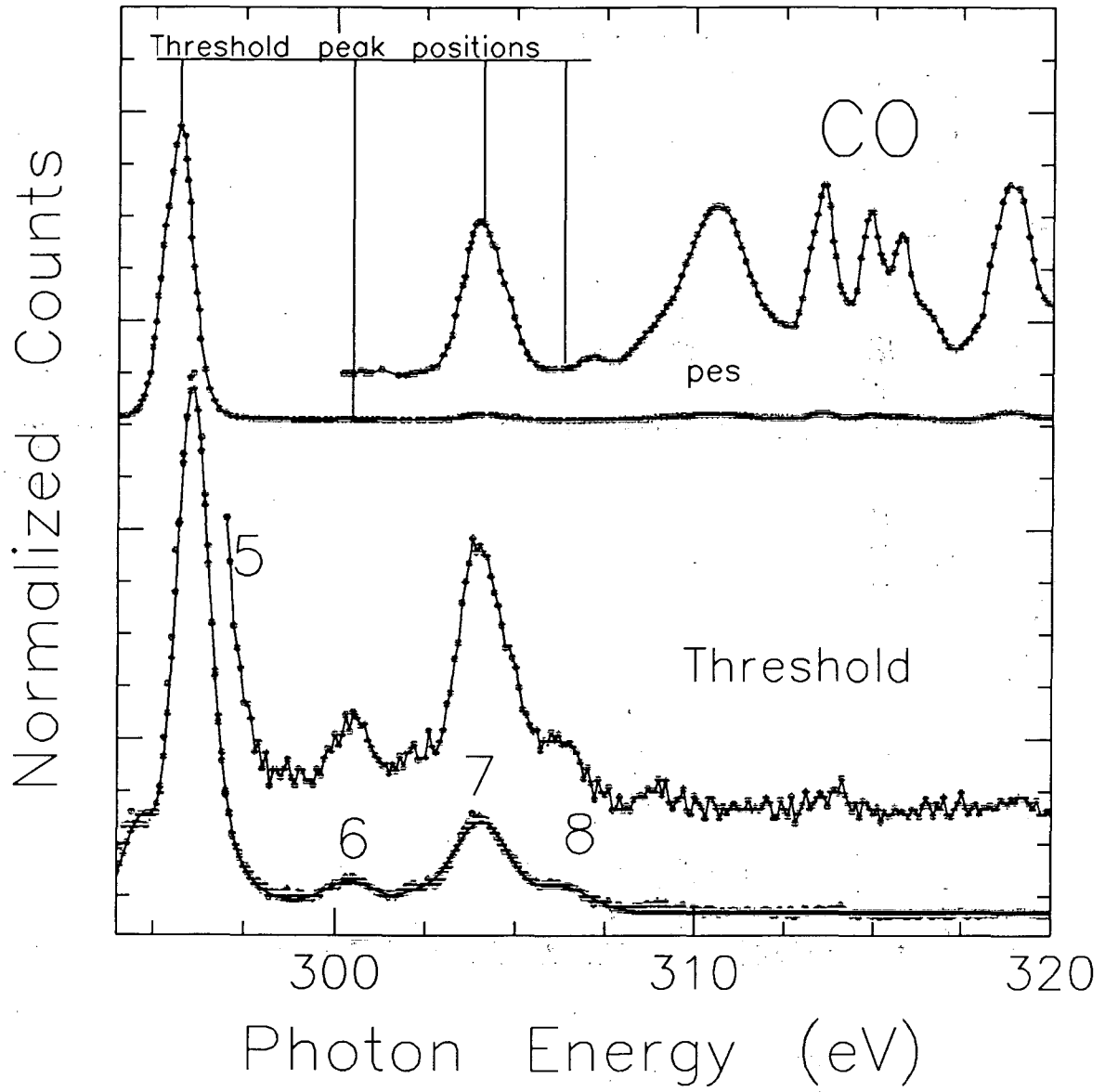


Figure 4

XBL 885-1919

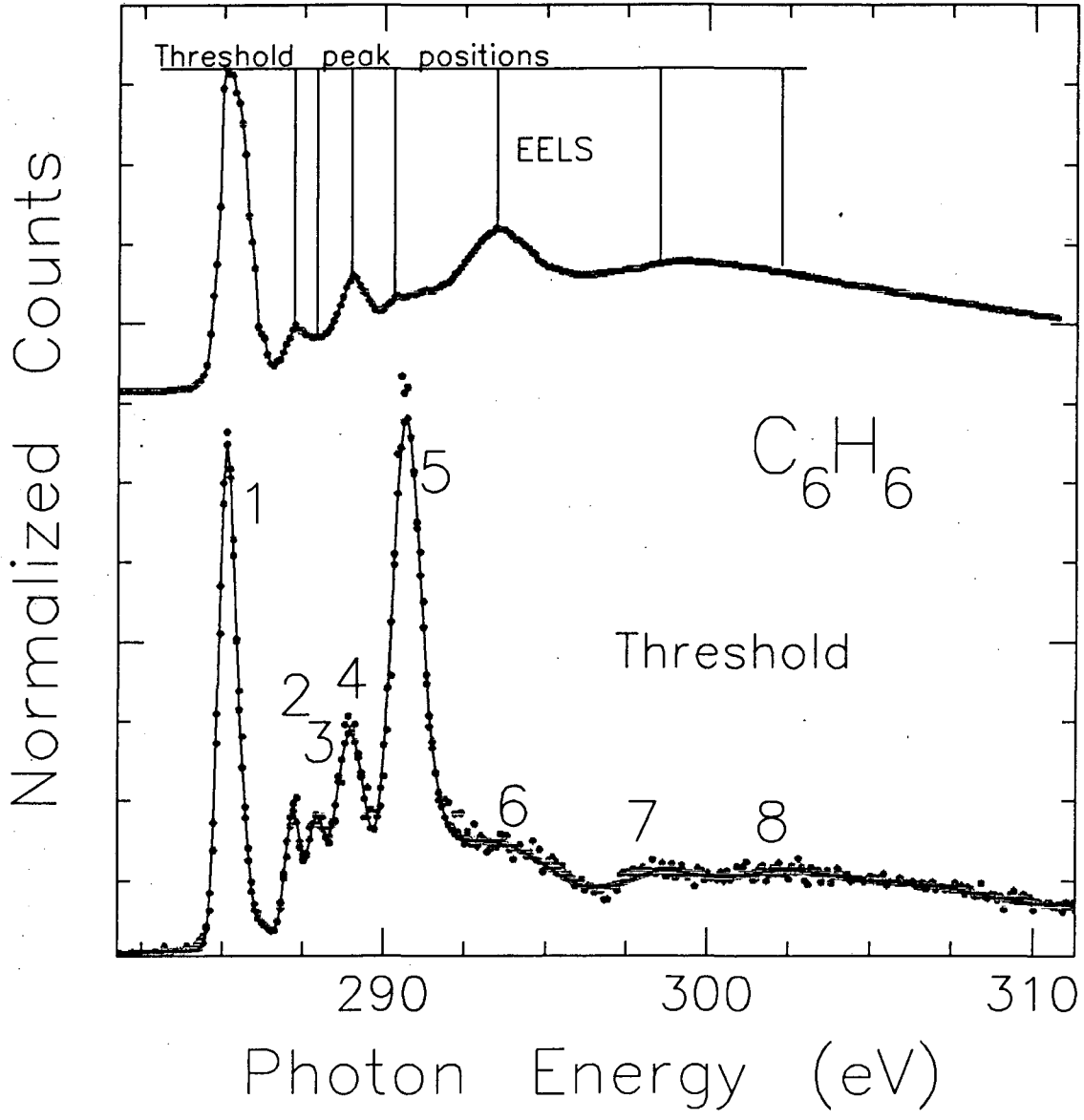
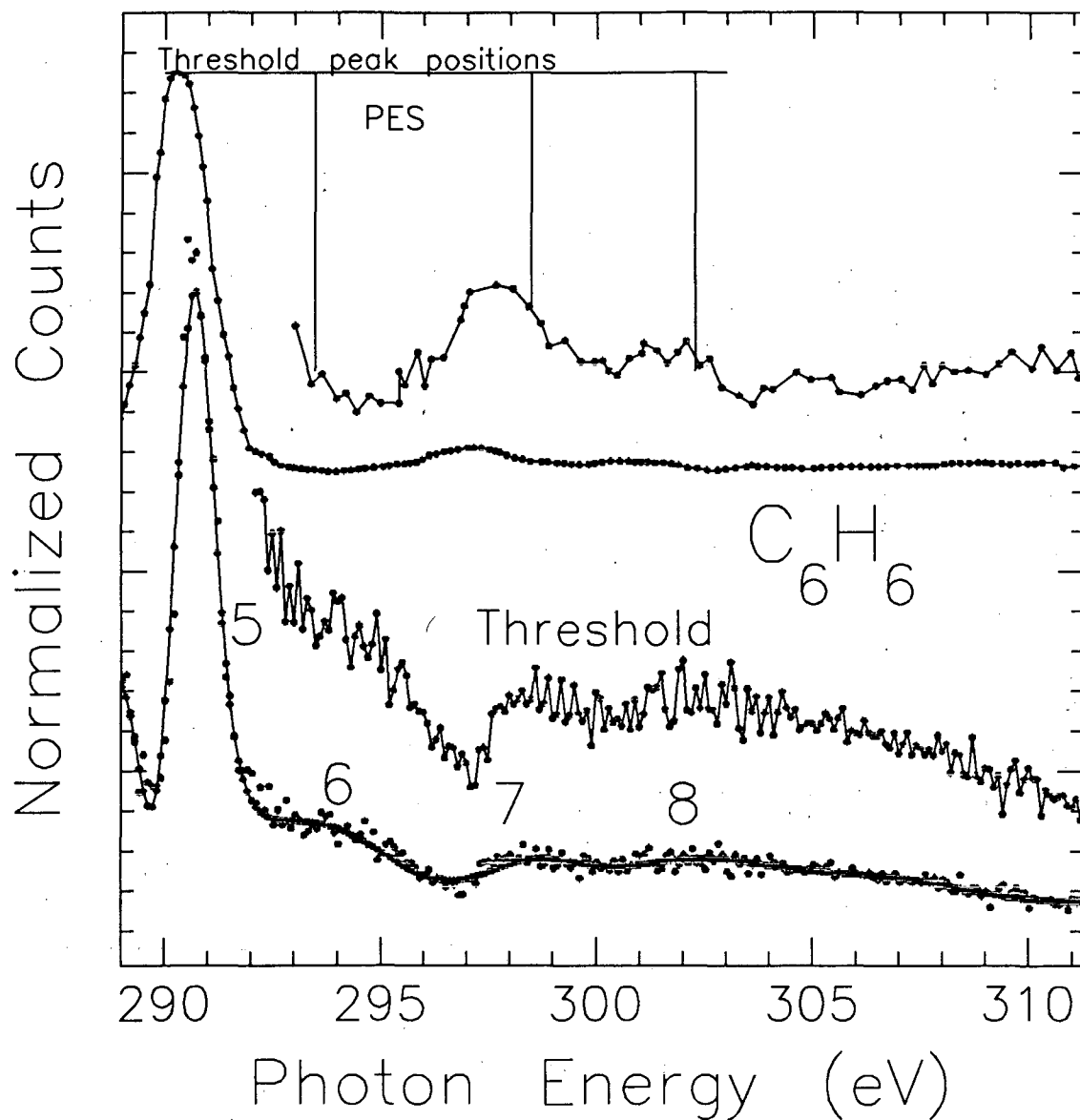


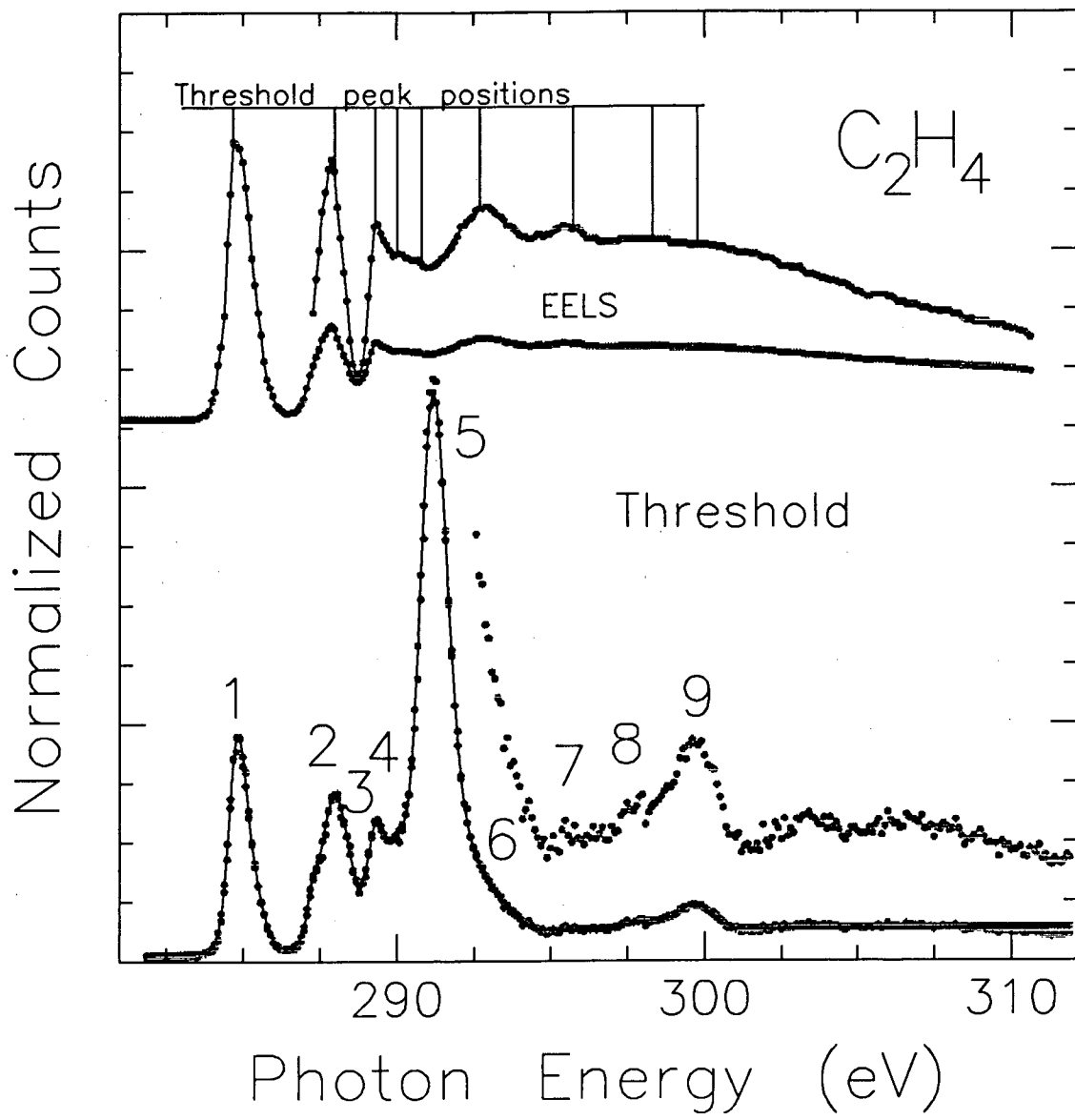
Figure 5

XBL 885-1920



XBL 885-1921

Figure 6



XBL 885-1922

Figure 7

*LAWRENCE BERKELEY LABORATORY  
TECHNICAL INFORMATION DEPARTMENT  
UNIVERSITY OF CALIFORNIA  
BERKELEY, CALIFORNIA 94720*